ACI STRUCTURAL JOURNAL TECHNICAL PAPER

Title no. 84-S6

Size Effect in Punching Shear Failure of Slabs

by Zdeněk P. Bažant and Zhiping Cao

Punching shear tests of geometrically similar reinforced concrete slabs of different sizes are carried out. The nominal shear stress at failure is not constant, as assumed in the current design formulas, but decreases as the slab size increases. The observed size effect in punching shear strength is approximately described by an improved design formula which uses the size-effect law for brittle failures due to distributed cracking. Applicability of this law is further supported by measurements of deflection diagrams, which reveal that the post-peak load decline becomes steeper as the slab size increases. Previous test data by various investigators are also analyzed collectively as one large set. Due to the enormity of scatter within this set, the absence of geometrical similarity and the lack of significantly different slab sizes within any single test series, these previous test data neither corroborate nor contradict the applicability of the size-effect law to punching shear.

Keywords: concrete slabs; cracking (fracturing); ductility; failure; **punching shear;** reviews; strains; structural design; **tests.**

Most current design formulas for failure loads of concrete structures are based on plastic limit analysis. Theoretically, plastic limit analysis is justified only if the load-deflection diagram terminates with a long horizontal yield plateau. During the 1970's, it nevertheless became popular to apply limit analysis to all types of failure, including various brittle failures, such as the punching shear failure. Recently this trend has been recognized to be unjustified. Brittle failures of concrete structures, which are characterized by a gradual decline of load at increasing deflection after the peak stress point, cannot be adequately described by plastic limit analysis because the failure does not occur simultaneously along the ultimate failure surface (except for very small structures). Rather, the failure is progressive, i.e., the failure zone propagates across the structure, with the energy dissipation localized into the cracking front. Thus, the failure load should be predicted by fracture mechanics, a theory which is based on energy and stability criteria instead of strength criteria. However, the classical, linear elastic fracture mechanics is normally inapplicable because the fracture front is not sharp but blunted by distributed cracking.[9,4]

The salient aspect of fracture mechanics is the size effect. Whereas for plastic limit analysis (as well as for the elastic allowable stress design) the nominal stress at failure of geometrically similar structures is size-independent, for fracture mechanics it decreases as the structure size increases. The classical, linear elastic fracture mechanics yields the strongest possible size effect, which is found to be excessive for most concrete structures. A new nonlinear form of fracture mechanics, approximately formulated as the blunt crack band model, yields a milder size effect, for which a simple size-effect law was derived by dimensional analysis and similitude arguments.[1] This size-effect law was shown to agree reasonably well with the test data from various types of fracture specimens[8].

In the current design codes, the formulas for the brittle failures of concrete structures ignore fracture mechanics and exhibit no size effect. However, in the preceding studies of diagonal shear failure of unprestressed and prestressed beams without stirrups,[7,5] of ring and beam failures of unreinforced pipes,[6] and of torsion failure of plain or longitudinally reinforced beams,[2] it has been found that the available test data exhibit a size effect describable by the size-effect law for blunt fracture. This corroborates the initial theoretical proposition that the size-effect law should apply, in an approximate sense, to all the brittle failures of concrete structures. The present study attempts to examine this proposition for the case of punching shear.

REVIEW OF SIZE-EFFECT LAW

Consider geometrically similar concrete structures of different characteristic sizes d, made of the same concrete. If their failure is purely brittle, i.e., if it is caused by concrete cracking, and if plastic energy dissipation during failure is negligible, then the nominal stress at failure approximately obeys the following size effect law (Fig. 1)

Received Oct. 7, 1985, and reviewed under Institute publication policies.
 Pertinent discussion will be published in the November-December *ACI Structural Journal* if received by July 1, 1987.

Zdeněk P. Bažant, FACI, is a professor and director, Center for Concrete and Geomaterials, Northwestern University. Dr. Bažant is a registered structural engineer, serves as consultant to Argonne National Laboratory and several other firms, and is on editorial boards of five journals. He is Chairman of ACI Committee 446, Fracture Mechanics, and a member of ACI Committee 209, Creep and Shrinkage in Concrete; 348, Structural Safety; and joint ACI-ASCE Committee 334, Concrete Shell Design and Construction. He also serves as Chairman of RILEM Committee TC69 on creep, of ASCE-EMD Committee on Properties of Materials, and of IA-SMiRT Division H. His works on concrete and geomaterials, inelastic behavior, fracture and stability have been recognized by a RILEM medal, ASCE Huber Prize and T. Y. Lin Award, IR-100 Award, Guggenheim Fellowship, Ford Foundation Fellowship, and election as Fellow of American Academy of Mechanics.

Zhiping Cao is a senior civil engineer and director, Center for Building Design, Design Institute, Yellow River Conservancy Commission, Zhengzhou, Henan Province, People's Republic of China. He has taken part in the planning of Yellow River Valley and several large hydraulic engineering projects. Mr. Cao spent the last two years as Visiting Scholar at the Center for Concrete and Geomaterials of Northwestern University, conducting both theoretical and experimental researches on the fracture mechanics applications and size effect in the failure of prestressed concrete beams, reinforced slabs, and pipes.

$$\sigma_N = B f_t' \phi(\lambda), \quad \phi(\lambda) = (1 + \frac{\lambda}{\lambda_0})^{-1/2} \qquad (1)$$

where $\sigma_N = P/bd$ where P = load at failure and b = thickness of structure; f_t' = direct tensile strength of concrete, d_a = maximum aggregate size, $\lambda = d/d_a$ = relative structure size; and B, λ_0 = empirical parameters characterizing the fracture energy of the material and the shape of the structure. This formula, which was derived by dimensional analysis and similitude arguments,[1] represents a gradual transition from the failure criterion of limit analysis (or allowable stress design) to the linear elastic fracture mechanics. The case of limit analysis, corresponding to a horizontal strength line in Fig. 1, is obtained for very small structures ($\lambda \ll \lambda_0 d_a$), and the case of linear elastic fracture mechanics, corresponding to a straight line of slope $-\frac{1}{2}$, is obtained for very large structures ($\lambda \gg \lambda_0 d_a$). Most practical structures represent the intermediate case, whereas most available laboratory data are near the limit analysis case ($\lambda \ll \lambda_0 d_a$).

The size-effect law was found to be in approximate agreement with the results of fracture tests of concrete. Furthermore, the test data available in the literature for diagonal shear failure of longitudinally reinforced nonprestressed as well as prestressed beams, for torsion failure of beams, and for beam and ring failures of pipes, were found to be in acceptable agreement[7,5,6,21] with the size-effect law although they could not be said to validate it, due to the large random scatter of the data.

Recently, it has been shown (see References 3 and 4 and the closure to Reference 7) that Eq. (1) represents the first order approximation to the most general size-effect law which reads $\sigma_N = B f_t' (\xi^{-1} + 1 + c_1\xi + c_2\xi^2 + c_3\xi^3 + \ldots)^{1/2r}$ where $\xi = (\lambda/\lambda_0 d_a)^r$; f_t', B, λ_0, r, c_1, c_2, . . . = constants. Furthermore, when d_a varies, f_t' varies, too, and approximately $f_t' = f_t^0 [1 + (c_0/d_a)^{1/2}]$, where f_t^0, c_0 = constants. However, these refinements of Eq. (1) are not used in the present study since they introduce further unknown parameters, the determination of which is impossible because of the high random scatter of the existing test data.

TEST SPECIMENS

To check the size effect, a series of tests of microconcrete specimens has been carried out. Three reinforced circular slabs for each of three different thicknesses d were cast, cured, and loaded to failure. The concrete mix ratio of cement:sand:gravel:water (by weight) was 1:2:2:0.5. The maximum aggregate size was d_a = ¼ in. (6.35 mm), and the maximum sand size was 1/16 in. (1.59 mm). The aggregate was crushed dolomitic limestone, the sand was river sand, and the portland cement was of ASTM Type I. The molds were made of plywood. A group of three specimens, one of each size, was cast one at a time from the same batch of concrete. Then each specimen was vibrated, and one day after casting the specimens were unmolded and placed for curing in a room with 90-percent relative humidity and 78 F (25.6 C) temperature. The specimens of Group I were moved from the humidity room to the laboratory [of temperature about 72 F (22.2 C) and relative humdity about 65 percent] one week before testing, and those of Groups II and III one day before testing. At the moment of test, the age of Groups I and II specimens was 228 days, and of Group III specimens 227 days. Three control cylinders of 3 in. (76.2 mm) diameter were cast from each batch of concrete and the uniaxial compressive strength f_c' was tested after standard 28-day curing; see Table 1. An orthogonal reinforcing mesh was placed at the bottom of each slab. For each group of specimens, the reinforcement ratio was slightly different so as to obtain at the same time some information on its possible effect, if any. None was detected, though. The average specific weights ρ of all slabs were determined by weighing each slab after the test in air and in water (Table 1), in order to check for a possible correlation with the measured nominal shear strength, which would make it possible to process the results to reduce scatter. However, no significant correlation has been found.

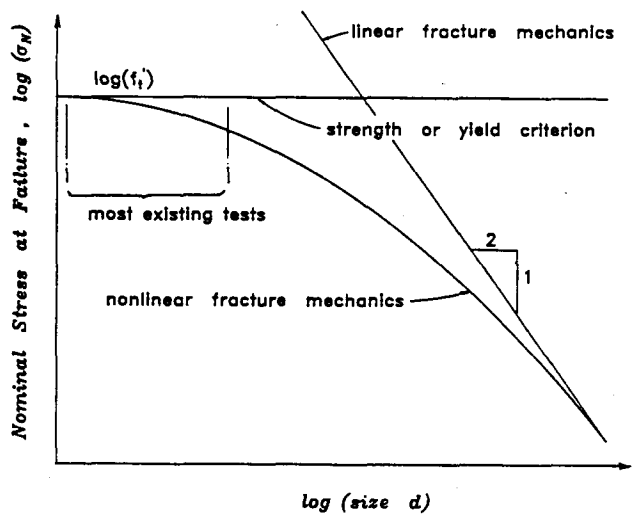

Fig. 1—Size-effect law for blunt fracture (dimensions in inches; 1 in. = 25.4 mm)

Table 1 — Data on the slabs tested

Group	Size	d (in.)	a (in.)	b (in.)	c_x (in.)	c_y (in.)	n_x	n_y	s_x (in.)	s_y (in.)	D_b (in.)	$\frac{f_y A_s d_x}{f'_c d^2}$	$\frac{f_y A_s d_y}{f'_c d^2}$	ρ, lb/ft³	f'_c (psi)	S.D.* of f'_c (psi)	v_u (psi)
I	A	1	5	1	0.156	0.269	13	19	0.340	0.267	0.113	0.0224	0.0247	188.10	7669	444	4.78
	B	2	10	2	0.325	0.575	10	14	0.873	0.738	0.250	0.0235	0.0237	172.38	7669	444	17.23
	C	4	20	4	0.650	1.15	10	14	1.746	1.476	0.500	0.0235	0.0237	171.42	7669	444	61.92
II	A	1	5	1	0.156	0.269	11	16	0.397	0.320	0.113	0.0192	0.0206	185.07	6953	267	5.05
	B	2	10	2	0.325	0.575	8	12	1.067	0.873	0.250	0.0193	0.0201	167.90	6953	267	17.70
	C	4	20	4	0.650	1.15	8	12	2.134	1.746	0.500	0.0193	0.0201	168.39	6953	267	69.60
III	A	1	5	1	0.156	0.269	9	13	0.476	0.400	0.113	0.0160	0.0165	184.04	7550	487	3.67
	B	2	10	2	0.325	0.575	6	10	1.372	1.067	0.250	0.0150	0.0164	161.49	7550	487	13.63
	C	4	20	4	0.650	1.15	6	10	2.744	2.134	0.500	0.0150	0.0164	162.51	7550	487	51.46

*S.D. = Standard deviation, based on three compression tests for each group (cylinders, 3 in. diameter), ρ = specific weight.
1 in. = 25.4 mm, 1 psi = 6895 Pa, 1 lb/ft³ = 16.02 kg/m³.

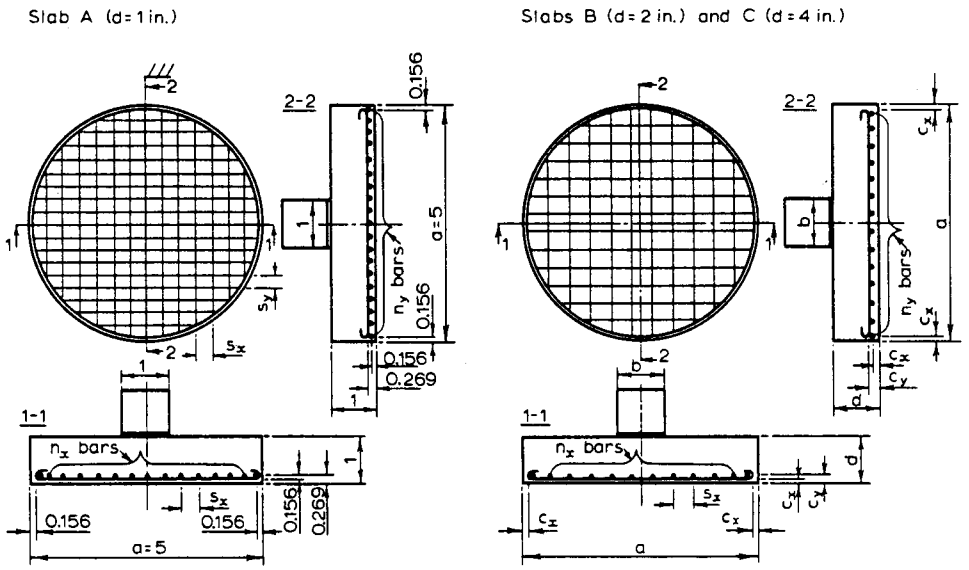

Fig. 2—Test specimens and their reinforcement

The slabs of size A had thickness d = 1 in. (25.4 mm), size B . . . 2 in. (50.8 mm), size C . . . 4 in. (101.6 mm). The slabs were designed so as to fail by punching shear rather than bending, and they did. The geometry of size A slabs is shown in Fig. 2 on the left and that of size B and C slabs in Fig. 2 on the right. All data on the slabs are given in Table 1 in which a = slab diameter, b = diameter of the circular flat steel punch; c_x, c_y = distances from the bottom face of the centroids of x- and y- direction bars; n_x, n_y = numbers of all x- and y-bars within the slab, D_b = bar diameter; and s_x, s_y = spacings of the x- and y-bars. Deformed bars of yield strength f_y = 45,000 psi (309 MPa) were used. The reinforcement mesh was rectangular (as close to square as possible). The spacings in x- and y-directions were slightly different to achieve a reinforcement that is approximately isotropic for bending, i.e., the moment of the bar yield force (per unit length) about the compression resultant is approximately the same for the x- and y-directions. The perimeter support consisted of a smooth continuous round steel bar bent into a circular shape. This type of support is not perfect, since radial horizontal friction forces can arise at the support; however, such forces have a negligible effect on the punching shear failure (although they may affect considerably the bending failure).

TESTING METHOD AND RESULTS

The slab specimens, simply supported in a horizontal position with span L such that L/a = 0.8, were loaded to failure in a closed-loop testing machine (MTS); see Fig. 3 and 4. The tests were displacement-controlled and the displacement rates were 0.002, 0.01, and 0.05 in./min. for the large, medium, and small specimens. For all specimen sizes, the maximum load was reached in about 5 min. The vertical displacement at the center of the slab on the bottom face was measured by an LVDT gage and used as a feedback signal for displacement control.

The typical load displacement diagrams are shown in Fig. 5. These diagrams exhibit a sharp peak followed by gradual softening. This confirms that the failure is caused mainly by brittle cracking of concrete, and not by plasticity of concrete, as assumed in many previous works. If the failures were caused by plasticity of concrete (or steel), the load-displacement diagram would have to exhibit a long horizontal plateau.

Note also that the larger the specimen, the steeper the decline of load after the peak point. It follows that the response of a larger specimen is more brittle (less ductile) than that of a smaller specimen, i.e., that the behavior of a larger specimen should be closer to linear elastic fracture mechanics and more different from a

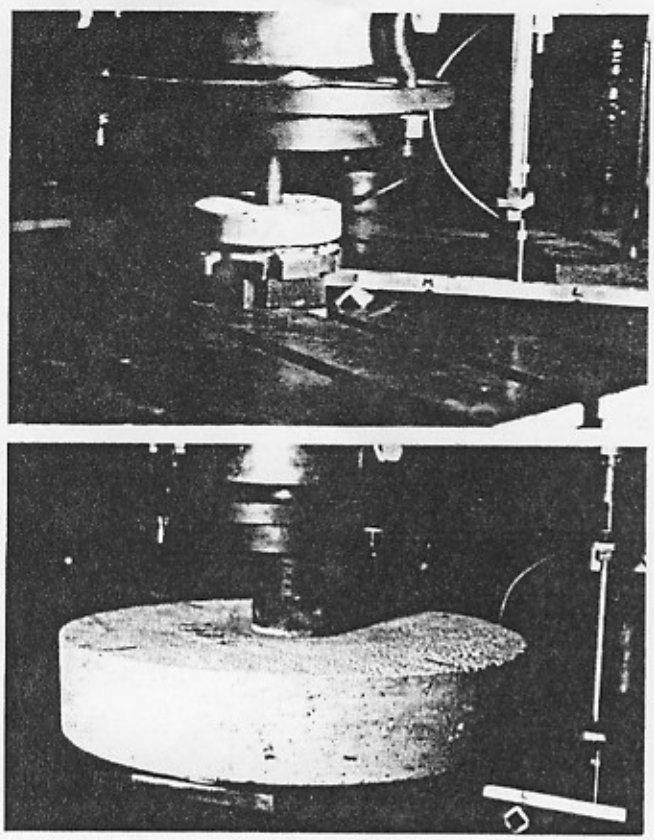

Fig. 3—Specimens in MTS testing machine

limit-analysis solution. This behavior represents an indirect confirmation of the size-effect law. For the largest specimen, the shape of the post-peak diagram is about the same as it is in direct tensile tests. From this, we may infer that the rate of plastic dissipation, as opposed to brittle cracking, is negligible in these failures.

Fig. 6 (d)-(f) shows the photographs of the bottom faces of the slabs after the tests (the cracks were marked by a pen for better visibility). The cracking patterns observed, typical of the punching shear failure, confirm that the cracking is quite distributed rather than localized. On the top face, by contrast, the deformation appears to be plastic [Fig. 6 (a) and (b)], due to confining compression stresses under the punch.

The test results are listed in terms of the nominal shear stress at failure v_u, defined as $v_u = P/\pi bd$ where P = maximum load measured, b = punch diameter, and d = slab thickness ($d = b$).

ANALYSIS OF TEST RESULTS

The formula currently used to predict punching shear failure[10,11,15,19] is

$$v_u = k_1 f'_c \left(1 + k_2 \frac{d}{b}\right) \qquad (2)$$

where k_1 and k_2 are empirical constants. This formula was derived theoretically by plastic limit analysis on the basis of the modified Coulomb yield criterion for concrete. The plastic failure surface (Fig. 4) closely resembles the observed final crack. Eq. (2), however, ex-

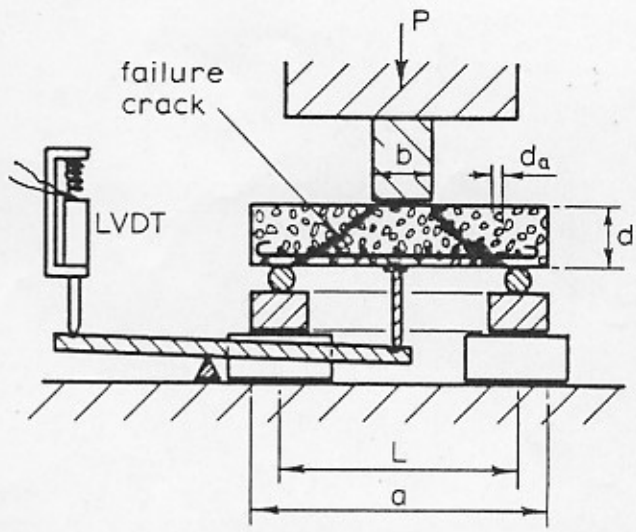

Fig. 4—Experimental setup and typical failure surface

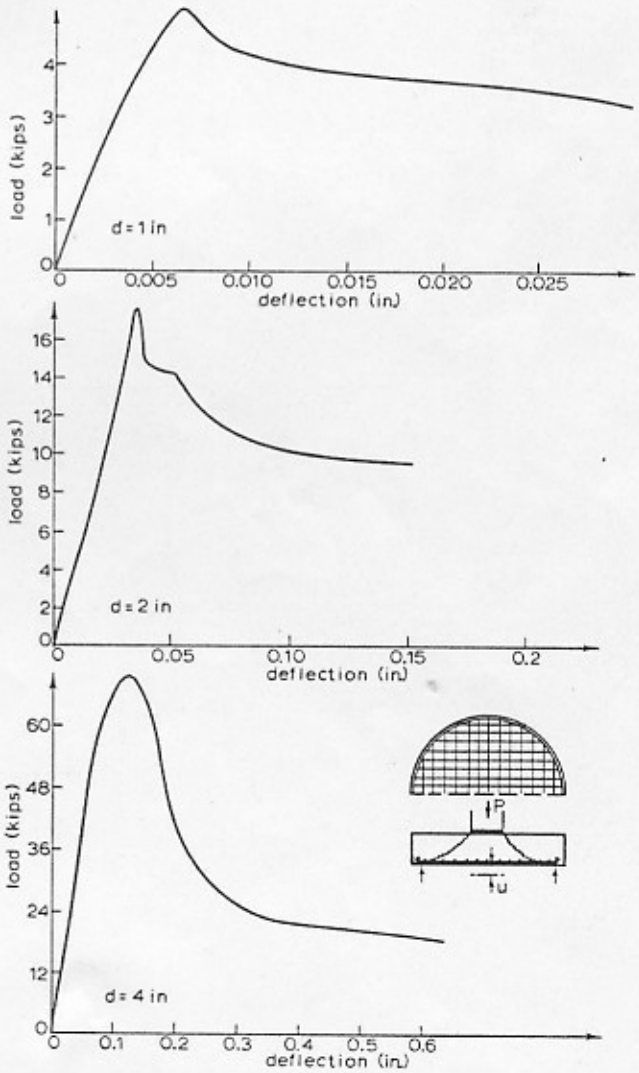

Fig. 5—Typical measured load-deflection diagrams for slabs of different thicknesses (1 kip = 6.895 MN, 1 in. = 25.4 mm)

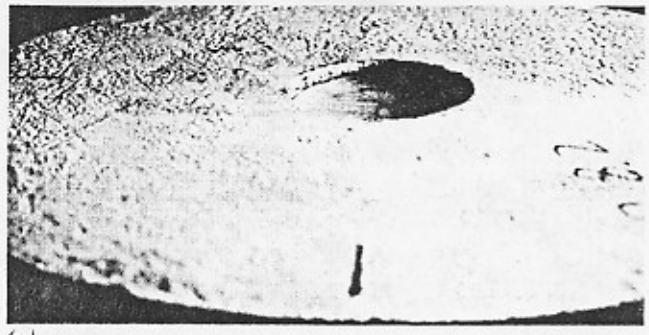

(a)

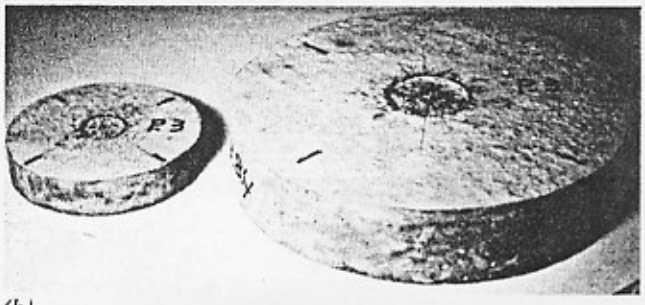

(b)

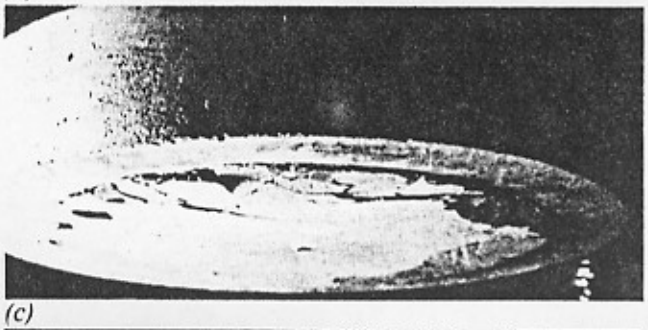

(c)

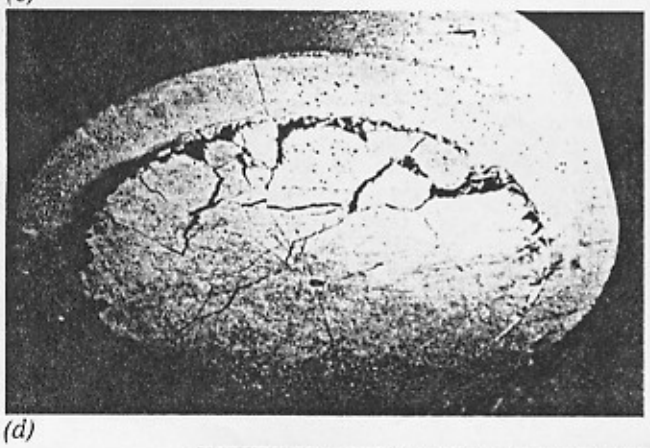

(d)

hibits no size effect. Since the failure is brittle rather than ductile, a size effect of the fracture mechanics type should be expected. Eq. (2) may then be generalized, in view of Eq. (1), as $v_u = C\phi\ (\lambda)$ or

$$v_u = C\left(1 + \frac{d}{\lambda_o d_o}\right)^{-1/2} \tag{3}$$

in which

$$C = k_1 f_t' \left(1 + k_2 \frac{d}{b}\right) \tag{4}$$

The coefficients in this relation may be easily determined by plotting $Y = v_u^{-2}$ versus $X = d/d_o$. According to Eq. (3), $Y = AX + D$ where $A = D/\lambda_0$, $D = C^{-2}$. Thus, the plot should ideally be linear, and linear regression may be applied.

The linear regression plots for the individual specimen groups tested are shown in Fig. 7(a), and for the entire set of measurements in Fig. 7(c). The corresponding size-effect plots are shown in Fig. 7(b) and (d). The parameter values for the optimum group fit in Fig. 7(c) and (d) are $\lambda_o = 28.5$, $k_1 = 0.155$. Fig. 7(c) also gives the linear regression statistics, consisting of the standard deviation (S.D.), the coefficient of variation $\omega_{\overline{Y}/X}$ for the deviations of the data points from the regression line, and of the mean data value $\overline{Y}$.

These figures show clearly that a size effect exists but is much weaker than linear fracture mechanics would indicate [slope $-\frac{1}{2}$ in Fig. 7(d)]. To make the size effect more conspicuous, the test results are replotted in Fig. 8 (a) and (b) in terms of the relative values of v_u with respect to the value for the smallest slab from the same batch of concrete.

The test results reveal no systematic effect of the reinforcement percentage. This agrees with the results of previous investigators as well as with the ACI formula.

EVALUATION OF TEST DATA FROM THE LITERATURE

The principal test data from the literature[12-14,16-18,20] were also examined for evidence of the size effect. Un-

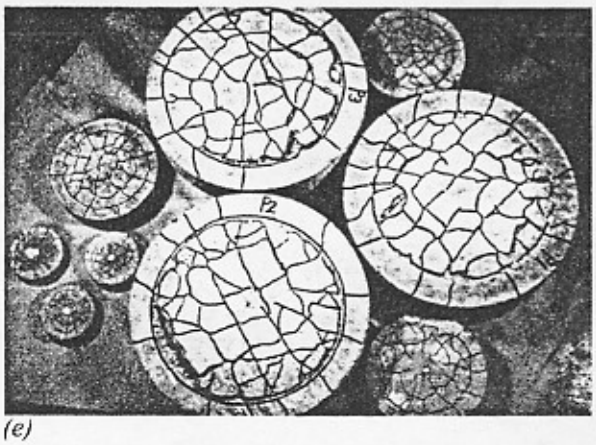

(e)

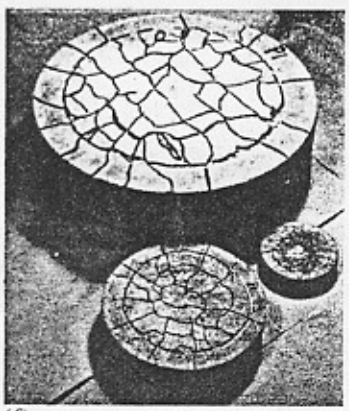

(f)

Fig. 6(a) through (f)—Specimens after test and their cracking pattern at bottom face

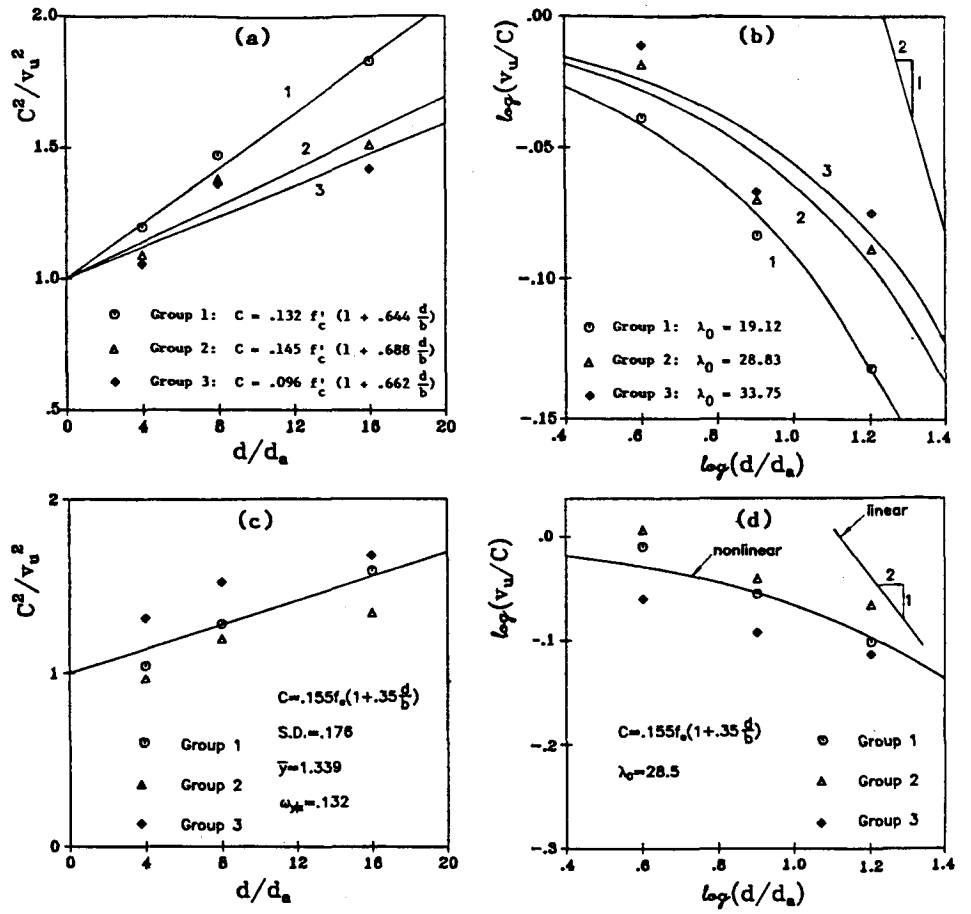

Fig. 7—Test results and their optimal fits

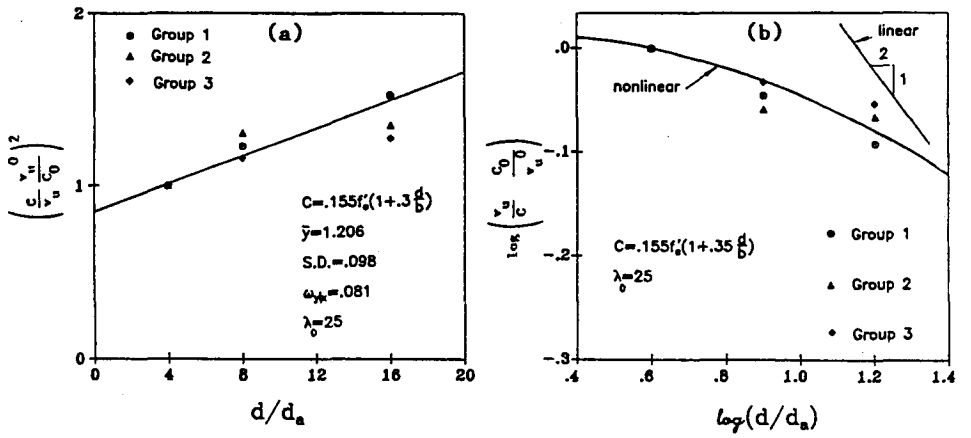

Fig. 8—Test results relative to the result for the smallest slab and their optimal fits

fortunately, not one of the previous test series included significantly different slab sizes. Nevertheless, in the set of all existing data, d/d_a ratios ranging from 4 to 12 were used by different investigators (Table 2). This suggests that a size effect might be detected by analyzing all data collectively, in the same manner as has been done with success for the diagonal shear failure of beams.[5,7]

The results of 159 tests by seven previous investigators[12-14,16-18,20] are plotted in Fig. 9(a) and (b). Basic information on these data is summarized in Table 2. The optimum fits of these data by Eq. (4) are also plotted in Fig. 9.

The comparisons in Fig. 9(a) and (b) do not contradict the size-effect law [or Eq. (3)], but neither do they corroborate it, because the scatter is enormous. The enormity of scatter is due to comparing the results from different laboratories obtained with different concretes and the results for slabs that were not geometrically similar. It was for this reason that the present tests were undertaken.

If the test results fitted the theory perfectly, the plot of the measured values versus the calculated values would lie on a straight line of Slope 1 passing through the origin. Thus, the deviations from this line are measures of the errors of the formula. Plots of this type are

Table 2 — Summary of previous test results

Slab No.	a, in.	d, in.	d_a, in.	d/d_a	L, in.	v_u, lb	f'_c, psi
Corley, Hawkins (1968)							
AN-1	40.00	5.75	0.750	7.67	336.00	75,100	2710
AH-3	40.00	5.75	0.750	7.67	336.00	91,200	3190
BN-1	40.00	5.75	0.750	7.67	336.00	59,700	2920
BC-1	40.00	5.75	0.750	7.67	336.00	71,800	2870
BH-1	40.00	5.75	0.750	7.67	336.00	88,500	2960
BH-2	40.00	5.75	0.750	7.67	336.00	67,700	2620
BH-3	40.00	5.75	0.750	7.67	336.00	90,400	3130
BN-1-P14	40.00	5.75	0.750	7.67	336.00	61,700	3680
BH-2-P14	40.00	5.75	0.750	7.67	336.00	60,600	2780
BH-3-P14	40.00	5.75	0.750	7.67	336.00	80,300	3100
BN-1-S14	40.00	5.75	0.750	7.67	336.00	54,800	3320
BH-2-S14	40.00	5.75	0.750	7.67	336.00	60,300	2960
BH-3-S14	40.00	5.75	0.750	7.67	336.00	84,200	3520
BN-1-S7	40.00	5.75	0.750	7.67	336.00	67,900	3700
BH-2-S7	40.00	5.75	0.750	7.67	336.00	77,700	3480
BH-3-S7	40.00	5.75	0.750	7.67	336.00	89,900	3740
Dragosavic, Van den Reukel (1974)							
1	9.44	1.40	0.315	4.44	58.75	7190	4450
2	9.44	1.40	0.315	4.44	58.75	7420	4450
3	9.44	1.40	0.315	4.44	58.75	5840	4450
4	9.44	1.40	0.315	4.44	58.75	4050	3190
5	9.44	1.40	0.315	4.44	58.75	7010	3210
6	9.44	1.40	0.315	4.44	58.75	6290	3210
7	9.44	1.40	0.315	4.44	58.75	7550	3430
8	9.44	1.40	0.315	4.44	58.75	8990	3720
9	9.44	1.40	0.315	4.44	58.75	7190	3720
10	9.44	1.40	0.315	4.44	58.75	3460	3610
11	9.44	1.40	0.315	4.44	58.75	4740	3610
12	9.44	1.40	0.315	4.44	58.75	5840	3420
13	9.44	1.40	0.315	4.44	58.75	5840	3420
14	9.44	1.40	0.315	4.44	58.75	7190	3420
15	9.44	1.40	0.315	4.44	58.75	7190	3420
16	9.44	1.40	0.315	4.44	58.75	7190	3420
Elstner, Hognestad (1956)							
A-1a	40.00	6.00	1.000	6.00	288.00	68,000	2040
A-1b	40.00	6.00	1.000	6.00	288.00	82,000	3660
A-1c	40.00	6.00	1.000	6.00	288.00	80,000	4210
A-1d	40.00	6.00	1.000	6.00	288.00	78,000	5340
A-1e	40.00	6.00	1.000	6.00	288.00	80,000	2940
A-2a	40.00	6.00	1.000	6.00	288.00	75,000	1980
A-2b	40.00	6.00	1.000	6.00	288.00	90,000	2830
A-2c	40.00	6.00	1.000	6.00	288.00	105,000	5430
A-2b	40.00	6.00	1.000	6.00	288.00	115,000	4050
A-3a	40.00	6.00	1.000	6.00	288.00	80,000	1850
A-3b	40.00	6.00	1.000	6.00	288.00	100,000	3280
A-4	56.00	6.00	1.000	6.00	288.00	90,000	3790
A-5	56.00	6.00	1.000	6.00	288.00	120,000	4030
A-6	56.00	6.00	1.000	6.00	288.00	112,000	3630
A-7	40.00	6.00	1.000	6.00	288.00	90,000	4130
A-8	56.00	6.00	1.000	6.00	288.00	98,000	3180
A-7a	40.00	6.00	1.000	6.00	288.00	63,000	4050
A-9	40.00	6.00	1.000	6.00	288.00	100,000	4330
A-10	56.00	6.00	1.000	6.00	288.00	110,000	4310
A-11	56.00	6.00	1.000	6.00	288.00	119,000	3760
A-12	56.00	6.00	1.000	6.00	288.00	119,000	4120
Kinnunen, Nylander (1960)							
3	18.55	5.94	1.250	4.76	211.50	50,490	3700
4	18.55	5.90	1.250	4.72	211.50	37,930	3810
5	18.55	5.87	1.250	4.69	211.50	57,330	3940
6	18.55	5.97	1.250	4.76	211.50	61,740	3860
7	18.55	6.02	1.250	4.81	211.50	55,570	4200
8	18.55	6.02	1.250	4.81	211.50	55,570	4200
9	18.55	5.90	1.250	4.72	211.50	61,740	3820
10	18.55	5.90	1.250	4.72	211.50	61,740	3820
11	18.55	6.02	1.250	4.81	211.50	74,970	4720
12	18.55	6.06	1.250	4.85	211.50	74,530	4550
13	18.55	5.90	1.250	4.72	211.50	42,340	4210
14	18.55	6.02	1.250	4.81	211.50	46,750	3810
15	18.55	6.10	1.250	4.88	211.50	42,340	3880
16	18.55	6.02	1.250	4.81	211.50	50,490	3930
17	18.55	6.02	1.250	4.81	211.50	51,160	3930
18	18.55	5.90	1.250	4.72	211.50	45,640	3990
19	18.55	5.84	1.250	4.69	211.50	44,540	4190
20	18.55	5.98	1.250	4.79	211.50	59,980	4000
21	18.55	5.90	1.250	4.72	211.50	63,950	3970
22	37.10	6.06	1.250	4.85	211.50	57,110	4160
23	37.10	5.94	1.250	4.76	211.50	46,750	4010
24	37.10	6.22	1.250	4.98	211.50	96,580	3880
25	37.10	6.06	1.250	4.85	211.50	91,730	3690
26	37.10	6.06	1.250	4.85	211.50	90,850	3880
27	37.10	6.06	1.250	4.85	211.50	79,820	3890
Kinnunen, Nylander (1960) (continued)							
28	37.10	5.94	1.250	4.76	211.50	82,690	3810
29	37.10	5.94	1.250	4.76	211.50	93,710	3810
30	37.10	5.94	1.250	4.76	211.50	110,250	4420
31	37.10	5.94	1.250	4.76	211.50	121,280	4420
32	37.10	6.10	1.250	4.88	211.50	57,990	3870
33	37.10	6.14	1.250	4.91	211.50	57,990	3920
34	37.10	5.90	1.250	4.72	211.50	74,530	4030
35	37.10	6.02	1.250	4.82	211.50	74,530	3680
36	37.10	5.98	1.250	4.79	211.50	63,060	3960
37	37.10	6.02	1.250	4.82	211.50	62,180	3950
38	37.10	6.02	1.250	4.82	211.50	79,820	4210
39	37.10	6.06	1.250	4.85	211.50	79,820	3930
40	37.10	6.02	1.250	4.82	211.50	67,250	3610
41	37.10	5.90	1.250	4.72	211.50	67,470	3880
42	37.10	6.02	1.250	4.82	211.50	85,330	4100
43	37.10	6.02	1.250	4.82	211.50	96,360	4030
Moe (1961)							
S1-60	40.00	6.00	0.375	12.00	288.00	87,500	3380
S2-60	40.00	6.00	0.375	12.00	288.00	80,000	3200
S3-60	40.00	6.00	0.375	12.00	288.00	81,750	3280
S4-60	40.00	6.00	0.375	12.00	288.00	75,000	3460
S1-70	40.00	6.00	0.375	12.00	288.00	88,200	3550
S3-70	40.00	6.00	0.375	12.00	288.00	85,000	3680
S4-70	40.00	6.00	0.375	12.00	288.00	84,000	5100
S4A-70	40.00	6.00	0.375	12.00	288.00	70,000	2970
S5-60	32.00	6.00	0.375	12.00	288.00	77,000	3220
S6-60	32.00	6.00	0.375	12.00	288.00	72,000	3110
S7-60	32.00	6.00	0.375	12.00	288.00	94,750	3340
S8-60	32.00	6.00	0.375	12.00	288.00	82,500	3340
S5-70	32.00	6.00	0.375	12.00	288.00	85,000	3340
S6-70	32.00	6.00	0.375	12.00	288.00	85,000	3520
M1A	37.70	6.00	0.375	12.00	288.00	97,300	3020
M2A	37.70	6.00	0.375	12.00	288.00	47,800	2250
M4A	37.70	6.00	0.375	12.00	288.00	32,300	2560
M2	37.70	6.00	0.375	12.00	288.00	65,700	3730
M3	37.70	6.00	0.375	12.00	288.00	46,600	3300
M6	31.40	6.00	0.375	12.00	288.00	53,800	3840
M7	31.40	6.00	0.375	12.00	288.00	70,000	3620
M8	31.40	6.00	0.375	12.00	288.00	33,600	3570
M9	31.40	6.00	0.375	12.00	288.00	60,000	3370
M10	31.40	6.00	0.375	12.00	288.00	40,000	3060
Mowrer, Vanderbilt (1967)							
M-2-1-0	16.00	3.00	0.750	4.00	192.00	19,300	4140
M-2-2-0	16.00	3.00	0.750	4.00	192.00	22,900	3610
M-3-1-0	24.00	3.00	0.750	4.00	192.00	17,800	3060
M-3-2-0_a	24.00	3.00	0.750	4.00	192.00	22,300	2610
M-3-2-0_b	24.00	3.00	0.750	4.00	192.00	38,600	7800
M-4-1-0	32.00	3.00	0.750	4.00	192.00	20,800	2250
M-4-2-0	32.00	3.00	0.750	4.00	192.00	29,800	3940
M-5-1-0	40.00	3.00	0.750	4.00	192.00	24,500	3380
M-5-2-0	40.00	3.00	0.750	4.00	192.00	34,100	3320
M-6-1-0	48.00	3.00	0.750	4.00	192.00	26,700	4060
M-6-2-0	48.00	3.00	0.750	4.00	192.00	35,600	3830
M-7-1-0	56.00	3.00	0.750	4.00	192.00	31,100	4020
M-7-2-0	56.00	3.00	0.750	4.00	192.00	41,500	3630
M-8-1-0	64.00	3.00	0.750	4.00	192.00	32,600	3610
M-8-2-0	64.00	3.00	0.750	4.00	192.00	41,500	3560
M-3-1-2	24.00	3.00	0.750	4.00	192.00	22,900	3920
M-3-1-4_a	24.00	3.00	0.750	4.00	192.00	22,300	3060
M-3-1-4_b	24.00	3.00	0.750	4.00	192.00	25,200	2900
M-3-2-4	24.00	3.00	0.750	4.00	192.00	23,700	2460
Taylor, Hayes (1965)							
1	8.00	3.00	0.375	8.00	140.00	8500	4260
2	8.00	3.00	0.375	8.00	140.00	8900	3760
3	12.00	3.00	0.375	8.00	140.00	13,000	4120
4	16.00	3.00	0.375	8.00	140.00	15,000	4120
5	20.00	3.00	0.375	8.00	140.00	11,950	3160
6	24.00	3.00	0.375	8.00	140.00	14,400	3160
7	8.00	3.00	0.375	8.00	140.00	7250	3760
8	8.00	3.00	0.375	8.00	140.00	8380	3760
9	12.00	3.00	0.375	8.00	140.00	9300	3560
10	12.00	3.00	0.375	8.00	140.00	11,500	3560
11	16.00	3.00	0.375	8.00	140.00	8750	3360
12	16.00	3.00	0.375	8.00	140.00	13,950	3360
13	20.00	3.00	0.375	8.00	140.00	9850	3200
14	20.00	3.00	0.375	8.00	140.00	14,500	3200
15	24.00	3.00	0.375	8.00	140.00	9850	2660
16	24.00	3.00	0.375	8.00	140.00	15,750	2660
17	8.00	3.00	0.375	8.00	140.00	8000	3300
18	8.00	3.00	0.375	8.00	140.00	8000	3300
19	16.00	3.00	0.375	8.00	140.00	11,750	3280
20	16.00	3.00	0.375	8.00	140.00	13,500	3280
21	24.00	3.00	0.375	8.00	140.00	15,300	3140
22	24.00	3.00	0.375	8.00	140.00	17,250	3140

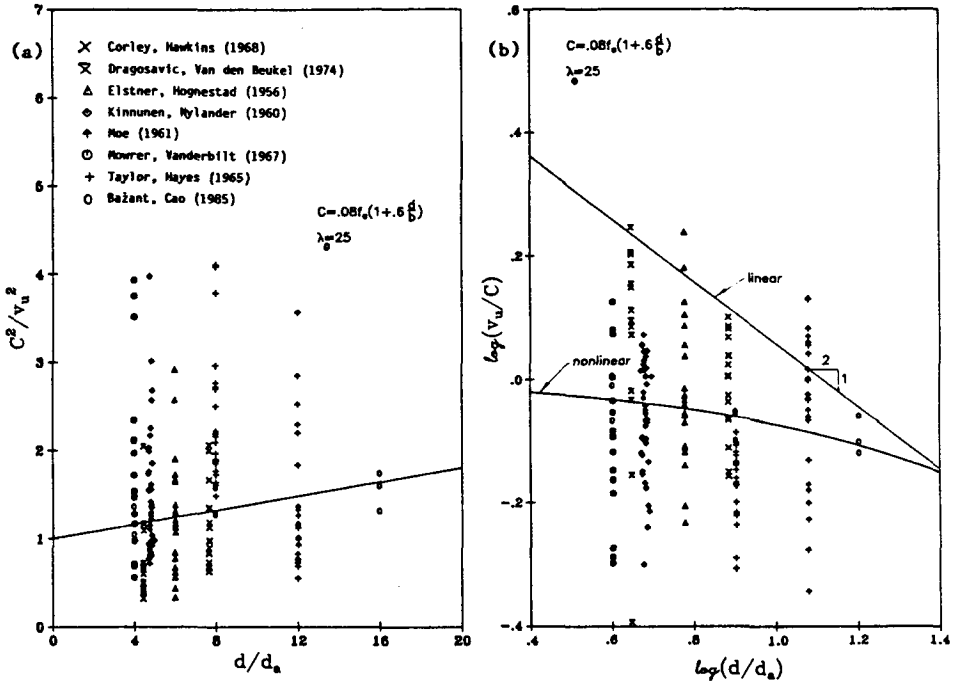

Fig. 9—Ultimate load data from the literature and optimal fit by size-effect law

shown in Fig. 10 (a) through (d) (where r is the correlation coefficient of regression). The theoretical values for the formulas of Elstner and Hognestad[14] and Moe[17] are given by $v_u = k_1 + k_2 f'_0$ (no effect of d/b) and $v_u = k_1 + k_3\, d/b)\, \sqrt{f'_c}$, respectively. (The latter formula is equivalent to that of ACI since $k_3 = k_1 k_2$.) The coefficient values for mean ultimate load predictions are $k_1 = 4.31$, $k_2 = 0.66$ for the ACI formula; $k_1 = 111.5$, $k_2 = 0.067$ for Elstner and Hognestad's formula[14] and $k_1 = 4.31$, $k_3 = 2.86$ for Moe's formula[17] ($2.86 = 4.31 \times 0.664$).

The comparisons of the data points with the theoretical lines (dashed) in Fig. 10 (a) through (c) show huge scatter, as indicated by the vertical deviations from the dashed line (the regression line is not plotted). The proposed formula [Eq. (4)] has only marginally better statistics than the previous formulas, and the comparison in Fig. 10(c) cannot be viewed at all as either a verification or an invalidation of Eq. (4) proposed here.

The design values v_u of nominal shear stress are obtained by applying to the formula a capacity reduction factor 0.75. The plots of such reduced nominal shear stress values versus the measured values are shown in Fig. 10 (d) through (f). In these plots, the majority of data are expected to lie above the theoretical straight line, as basically they do, although a few data points still fall dangerously low below the prediction line. This happens even when the size effect is introduced [Fig. 10(f)]; the variation coefficient and the correlation coefficient are only marginally better for this graph [Fig. 10(f)].

The scatter of the data points in Fig. 10 is very large. Apparently, aside from the effects of b/d and size, there are some other systematic influences which are not yet understood.

CONCLUSIONS

1. The punching shear failure of slabs without stirrups is not plastic but brittle. This is evidenced by the fact that, after the peak, the load-deflection diagram exhibits a gradual decline rather than a plastic yield plateau. Due to the brittleness of failure, the size-effect law for blunt failures should, in theory, apply.

2. The punching shear tests of geometrically similar concrete slabs of different sizes, carried out as part of the present investigation, indicate that the size effect exists, i.e., the nominal stress at failure decreases as the size increases. These new test results show acceptable agreement with the size-effect law, and lead to an improved design formula [Eq. (3)].

3. The larger the slab thickness, the steeper the post-peak decline of the load-deflection diagram; thus, the punching shear behavior of thin slabs is closer to plasticity, and that of thick slabs is closer to linear elastic fracture mechanics. This independently confirms the applicability of the size-effect law, since this law predicts exactly such kind of behavior.

4. Previous test data from the literature do not contradict the proposed formula but they do not validate it either, due to their enormous scatter when they are all analyzed collectively.

5. In view of the limited number of tests, the not very broad size range, and the use of small aggregate (maximum size ¼ in. or 6.35 mm), it would be desirable to conduct further geometrically similar size-effect tests with much larger slabs and a regular-size aggregate (this would of course require much larger funding).

ACKNOWLEDGMENT

The fundamental investigations underlying the present work were supported by U.S. Air Force Office of Scientific Research under Grant No. 83-0009.

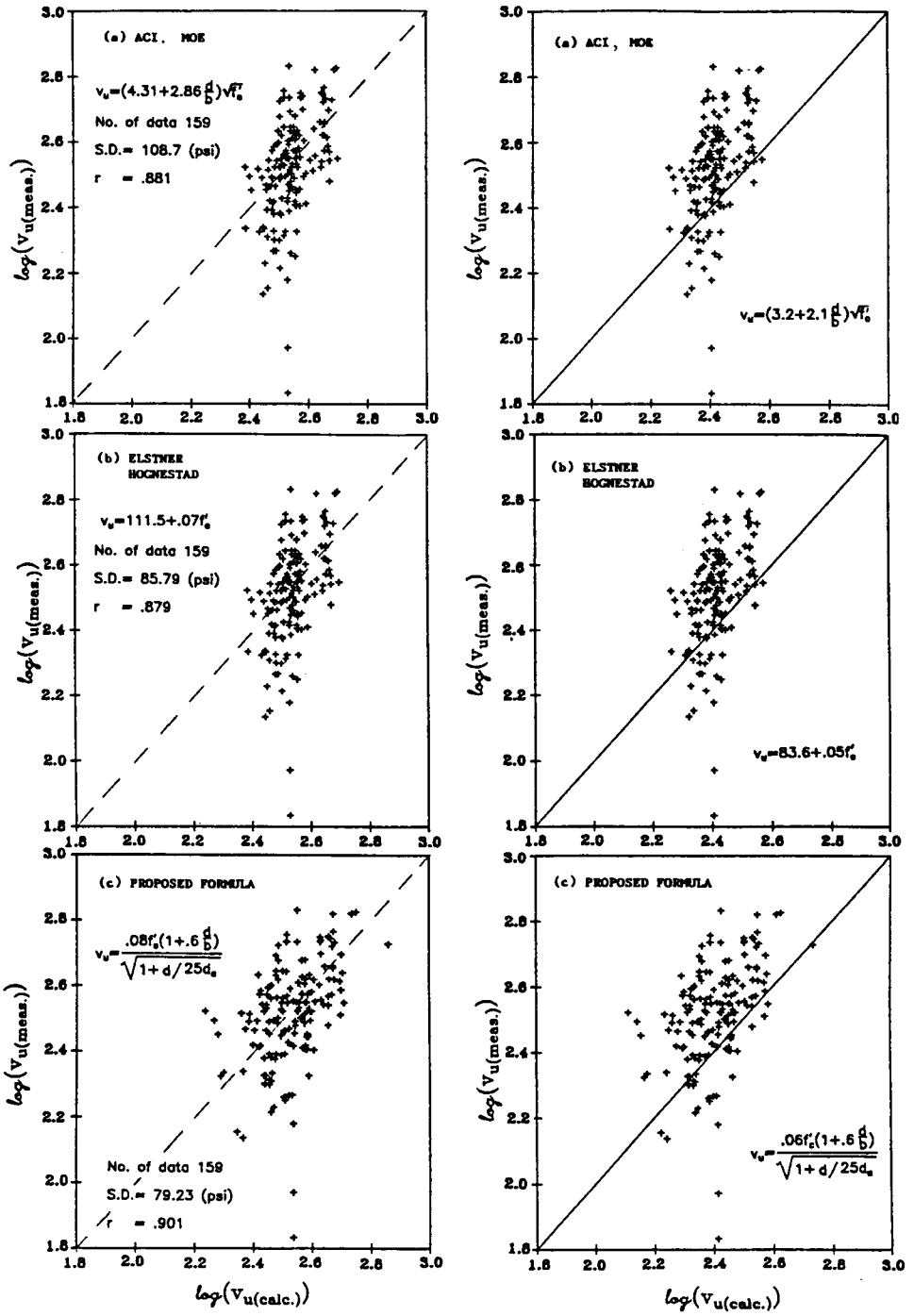

Fig. 10—Plot of measured versus calculated nominal shear strength values at ultimate load: left—mean formula; right—design formula

REFERENCES

1. Bažant, Zdeněk P., "Size Effect in Blunt Fracture: Concrete, Rock, Metal," *Journal of Engineering Mechanics,* ASCE, V. 110, No. 4, Apr. 1984, pp. 518-535.

2. Bažant, Z. P., "Mechanics of Fracture and Progressive Cracking in Concrete Structures," *Fracture Mechanics of Concrete: Structural Application and Numerical Calculation,* Martinus Nijhoff Publishers, Dordrecht-Boston, 1985, pp. 1-94.

3. Bažant, Zdeněk P., "Comment on Hillerborg's Comparison of Size Effect Law and Fictitious Crack Model," *Dei Poli Anniversary Volume,* Politecnico di Milano, 1985, pp. 335-338.

4. Bažant, Z. P., "Fracture Mechanics and Strain-Softening of Concrete," *Proceedings,* U.S.-Japan Seminar on Finite Element Analysis of Reinforced Concrete Structures, Japan Concrete Institute, Tokyo, 1985, pp. 47-69. Also in *Proceedings,* ASCE, New York, pp. 121-150; and as "Mechanics of Distributed Cracking," *Applied Mechanics Reviews,* V. 39, No. 5, May 1986, pp. 675-705.

5. Bažant, Zdeněk P., and Cao, Zhiping, "Size Effect of Shear Failure in Prestressed Concrete Beams," ACI JOURNAL, *Proceedings* V. 83, No. 2, Mar.-Apr. 1986, pp. 260-268.

6. Bažant, Zdeněk P., and Cao, Zhiping, "Size Effect in Brittle Failure of Unreinforced Pipes," ACI JOURNAL, *Proceedings* V. 83, No. 3, May-June 1986, pp. 369-373.

7. Bažant, Zdeněk P., and Kim, Jin-Keun, "Size Effect in Shear Failure of Longitudinally Reinforced Concrete Beams," ACI JOURNAL, *Proceedings* V. 81, No. 5, Sept.-Oct. 1984, pp. 456-458. Also, Discussion, V. 82, No. 4, July-Aug. 1985, pp. 579-583.

8. Bažant, Zdeněk P.; Kim, Jin-Keun; and Pfeiffer, Phillip A., "Nonlinear Fracture Properties from Size Effect Tests," *Journal of*

Structural Engineering, ASCE, V. 112, No. 2, Feb. 1986, pp. 289-307.

9. Bažant, Zdeněk, and Oh, B. H., "Crack Band Theory for Fracture of Concrete," *Materials and Structures, Research and Testing* (RILEM, Paris), V. 16, No. 93, May-June 1983, pp. 155-177.

10. Braestrup, M. W., "Punching Shear in Concrete Slabs," Lic. Techn. thesis, Structural Research Laboratory, Technical University of Denmark, Lyngby, 1976.

11. Chen, Wai-Fah, *Plasticity in Reinforced Concrete,* McGraw-Hill Book Co., New York, 1982, pp. 329-332.

12. Corley, W. Gene, and Hawkins, Neil M., "Shearhead Reinforcement for Slabs," ACI JOURNAL, *Proceedings* V. 65, No. 10, Oct. 1968, pp. 811-824.

13. Dragosavic, M., and Van den Beukel, A., "Punching Shear," *Heron* (Delft), V. 20, No. 2, 1974, 48 pp.

14. Elstner, Richard C., and Hognestad, Eivind, "Shearing Strength of Reinforced Concrete Slabs," ACI JOURNAL, *Proceedings* V. 53, No. 1, July 1956, pp. 29-58.

15. Hess, U., and Jensen, B. C., "Gennemlokning af jernbeton plader," *Report* No. R90, Structural Research Laboratory, Technical University of Denmark, Lyngby, May 1978, 63 pp.

16. Kinnunen, S., and Nylander, H., "Punching of Concrete Slabs without Shear Reinforcement," *Transactions,* Royal Institute of Technology, Stockholm, 1960, 110 pp.

17. Moe, Johannes, "Shear Strength of Reinforced Concrete Slabs and Footings Under Concentrated Load," *Development Department Bulletin* No. D47, Portland Cement Association, Skokie, 1961, 135 pp.

18. Mowrer, R. D., and Vanderbilt, M. D., "Shear Strength of Lightweight Aggregate Reinforced Concrete Flat Plates," ACI JOURNAL, *Proceedings* V. 64, No. 11, Nov. 1967, pp. 722-729.

19. Nielsen, M. P.; Braestrup, M. W.; Jensen, B. C.; and Bach, F., "Concrete Plasticity. Beam Shear—Shear in Joints—Punching Sheear," *Special Publication,* Danish Society for Structural Science and Engineering, Copenhagen, 1978, 129 pp.

20. Taylor, R., and Hayes, B., "Some Tests on the Effect of Edge Restraint on Punching Shear in Reinforced Concrete Slabs," *Magazine of Concrete Research* (London), V. 17, No. 50, Mar. 1965, pp. 39-44.

21. Bažant, Z. P., and Sener, S., "Size Effect in Torsional Failure of Beams," *Report* No. 86-8/428, Center for Concrete and Geomaterials, Northwestern University, Evanston, Aug. 1986, 21 pp.